Supporting Information

Heat Treatment Mechanism in Regulating the Self-Discharge Behavior of Li/CF_x Primary Batteries

Yiling Huang[+,a] Ziqiang Fan[+,a] Zhida Chen[+,a] Zhiguo Li,[b] Wei Yang,[b] Alice A. Kasera,[c] Caiting Lai,*[b] Zhongzhi Yuan,*[a] Ronghua Zeng,*[a]

a. Guangdong Provincial International Joint Research Center for Energy Storage Materials, National and Local Joint Engineering Research Center of MPTES in High Energy and Safety LIBs, School of Chemistry, South China Normal University, Guangzhou 510006, China.

b. EVE Energy Co. Ltd, Huizhou, Guangdong 516006, China.

c. School of Engineering, Mount Kenya University, Thika 342-01000, Kenya.

+ These authors contributed equally: Yiling Huang, Ziqiang Fan, Zhida Chen.

Materials and Methods

The cathode material was CF01 (FHC), produced by the fluorination of biomass-derived carbon (Xiamen ZKXifu Technology Co., Ltd., Xiamen, China). A reactor containing CF01 was subjected to heat treatment in a nitrogen atmosphere. Nitrogen was first introduced to purge the air from the reactor, and the reactor was then heated to a target temperature of 250-350 °C at a rate of 10 °C min, with a dwell time of 5 h at the desired temperature. The starting material was modified at varying heat treatment conditions and denoted as CF02 (FHC@250°C), CF03 (FHC@300°C), and CF04 (FHC@350°C) for the treatment at 250, 300, and 350 °C, respectively.

The electrode preparation comprised five steps: material mixing, slurry homogenization, coating, drying, and cutting. Although FHC exhibits improved electronic conductivity relative to commercial fluorinated graphite, its absolute conductivity is still low, requiring a higher percentage of conductive additive for practical application. So, FHC, conductive carbon black, and polyvinylidene fluoride binder were weighed and combined in a ball-milling jar to completely homogenize them. The electrode slurry consisted of 80 wt.% of the electrically active FHC and 10 wt.% of conductive carbon black. The materials were quickly mixed in the jar, and a suitable quantity of N-methyl-2-pyrrolidone (NMP) solvent was added together with the fluorinated carbon powder. The slurry was further ball-milled to obtain a uniform, homogenous mixture of suitable viscosity. Afterward, this slurry was applied to an 8 μm thick carbon-coated aluminum foil using an adjustable film coater (model KTQ-150-SB, MTI Corporation) to generate a large electrode sheet. The coated sheet was placed flat in a vacuum oven and dried at 90 °C for 12 h to remove the solvent completely. Once the drying process was finished, the electrode sheet was subjected to high-pressure rollers at 20 MPa for 10 s to increase its density and improve electrical contact. Ultimately, the pressed electrode was cut into disks with a 12 mm diameter using a precision cutting machine. The electrode discs contained about 5 to 6 mg/cm² of active material, giving an electrode density of about 1.3 g/cm³, which is proper for coin cell assembly.

Coin cells (type BR2025) were assembled in an Ar-filled glove box (p_{H_2O} < 0.01 ppm, p_{O_2} < 0.01 ppm). Metal lithium was used as the anode material. The electrolyte solution consisted of 1.0 M $LiBF_4$ mixed with propylene carbonate (PC) and 1,2-dimethoxyethane (DME) in a volume ratio of 1:1 (all supplied by Shenzhen CAPCHEM Technology Co., Ltd.). A dry-process polypropylene (PP) separator (SENIOR, thickness: 16 μm, diameter: 19 mm) was placed between the electrodes. The assembly procedures were conducted under the controlled Ar atmosphere.

X-ray diffraction (XRD) analysis was performed using a Rigaku SmartLab diffractometer with Cu Kα radiation (λ = 1.54056 Å) in a 2θ range from 10 to 80° at a scan rate of 10 °/min.

The surface morphology of materials and electrodes was examined by scanning electron microscopy (SEM, JEOL JSM-7610FPlus). We used energy-dispersive X-ray spectroscopy (EDS) to determine the atomic composition on the surface, while the chemical states were determined by X-ray photoelectron spectroscopy (XPS, Thermo Scientific Nexsa) with a monochromatic Al-Kα X-ray source. Nitrogen adsorption analysis was performed on a physical adsorption analyzer (Micromeritics ASP-2020 M) to measure the specific surface area. The chemical structure and bond types were analyzed by Fourier-transform infrared spectroscopy (FT-IR, Thermo Scientific Nicolet iS20).

The Neware battery test system was used to conduct galvanostatic discharge tests on BR2025 coin cells in a temperature-controlled chamber at 25±1 °C. The BR2025 coin cells were discharged at a rate of 0.01C, and the discharge process was stopped when the voltage reached 1.5 V. Linear sweep voltammetry (LSV) was performed using a CHI660D electrochemical workstation (Chenhua) starting from the open-circuit voltage and ending at 1.5 V, at a scanning rate of 0.5 mV/s. To study the self-discharge performance, the irreversible capacity loss rate was measured after storing the cells at 55 °C for 7 consecutive days.

Supplementary Discussion about the influence of the heat treatment process on electrochemical properties of Li/CF_x batteries

The corresponding capacity loss of Li/CFx batteries can be attributed to the reduction reaction to which fluorinated carbon (CF_x) as the cathode material undergoes change during discharge process, as shown in Equation (1):

$$CFx + xLi = C + xLiF\#(1)$$

Here, a variable theoretical specific capacity Q (in $mAh \cdot g^{-1}$) of CF_x depends on its fluorination degree (x) according to Eqs. (2) and (3):

$$Q = xF/3.6M\#(2)$$

$$M = 12 + 19x\#(3)$$

According to above Eqs., the electrochemical properties of CF_x materials are associated with the F/C ratio. A lower fluorine concentration is considered to be linked with a greater power density and a comparatively lower specific capacity, whereas an increased fluorine concentration is expected to raise Q at the expense of specific power[1]. In the given experiments, the untreated CF01 sample exhibited the highest specific capacity of all four materials used, similar to the calculated values. The heat-treated samples (CF02, CF03, and CF04) exhibited a reduction in the F/C ratio compared to CF01. The Q value decreases as the F/C ratio becomes lower, as shown above. The practical specific capacities of CF02 and CF03 were also reduced, while that of CF04 is higher than that of CF02 and CF03, which could be explained by the fact that CF04 has more defects and active sites that initiate the reaction and provide a slight increase in the specific capacity.

The pouch-cell tests further verify the reproducibility and practical effectiveness of the heat-treatment strategy. The initial discharge capacities of CF01 and CF03 were 4.24 Ah and 4.22 Ah, respectively. Three independent pouch cells were tested for each sample, and a high consistency in discharge capacity was observed, indicating good reproducibility of the cell fabrication and electrochemical performance. After storage, the discharge capacities of CF03 and CF01 were 4.20 Ah and 3.97 Ah, respectively. Correspondingly, the capacity retentions were calculated to be 99.53% for CF03 and 93.63% for CF01. These results demonstrate that heat treatment effectively improves the storage stability of Li/CF_x primary batteries, leading to a 5.9% enhancement in capacity retention compared with the untreated cell.

The gravimetric energy density was evaluated based on the total mass of the pouch cell (27.6 g), as summarized in Tab. 3. At a low discharge rate of 0.01 C, the CF01 cell delivered an energy output of 13.11 Wh, corresponding to a gravimetric energy density of 474.6 Wh kg^{-1}, while CF03 exhibited a slightly lower value of 468.7 Wh kg^{-1} with a discharge energy of 12.94 Wh.

When the discharge rate increased to 0.5 C, both cells maintained comparable energy outputs (11. 588 and 11.594 Wh for CF01 and CF03, respectively), yielding stable gravimetric power densities after normalization to the total cell mass. The corresponding average discharge voltages at 0.5 C were 2.73 V for CF01 and 2.74 V for CF03, indicating similar polarization behavior under elevated current conditions. The combination of stable discharge voltage and preserved energy output demonstrates that the heat-treated CF_x cathodes effectively maintain a favorable balance between energy and power performance.

Reference

1 P. Chen, B. Wang, Z. Wu, X. Niu, C. Ouyang, H. Li and L. Wang, *J. Energy Chem*., 2023, **77**, 38.

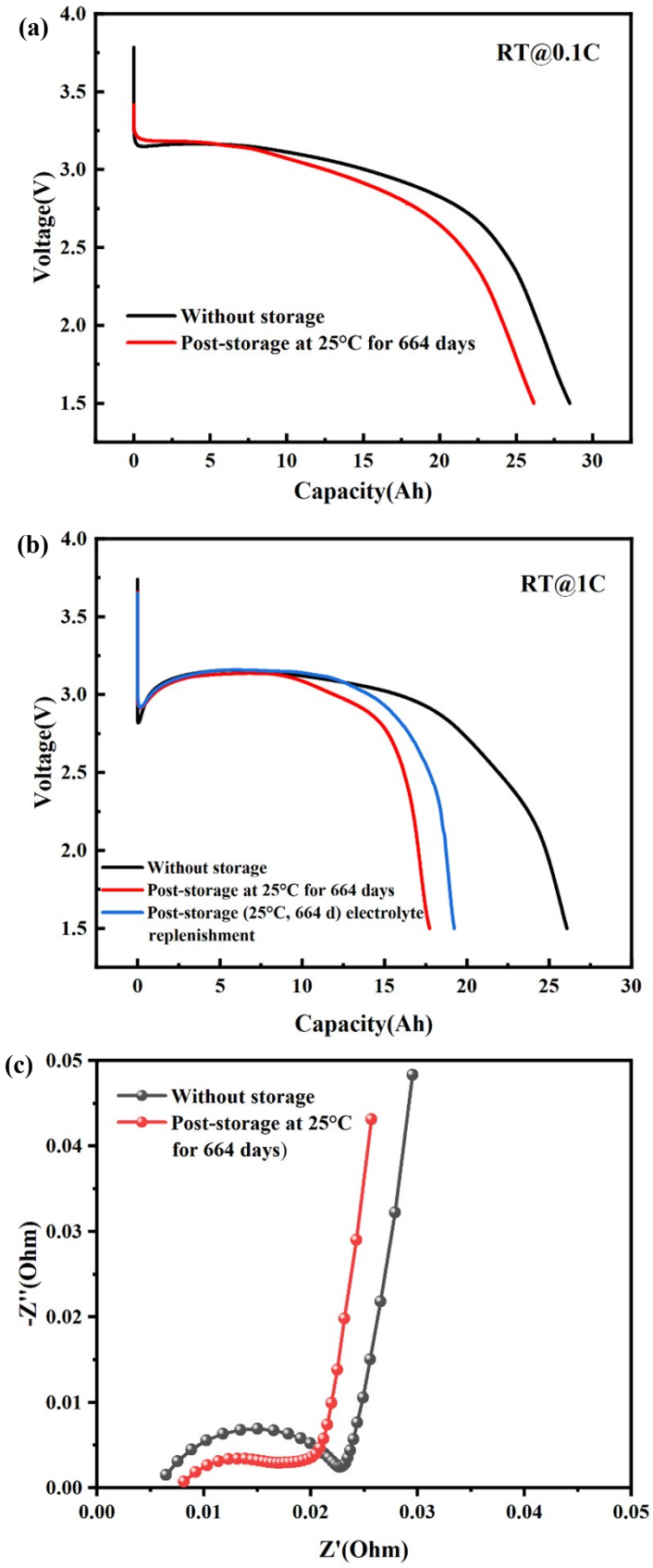

Fig. S1. (a) Constant-current discharge curves at 0.1C, (b) Constant-current discharge curves at 1C, and (c) EIS Nyquist plots for fresh and room-temperature-stored (664 days).

Fig. S2 shows the macroscopic appearance and color of CF01, CF02, CF03, and CF04. Fig. S3 shows the surface F/C ratios of CF01, CF02, CF03, and CF04, being 0.9, 0.81, 0.79, and 0.65, respectively. While CF01, which has the greatest F/C ratio, exhibited a brown-yellow color, the CF02, CF03, and CF04 samples became darker in the respective order. As the F/C ratio decreases, the CF_x materials exhibit a gradual darkening in color.

Fig. S2. Optical images of the materials after heat treatment.

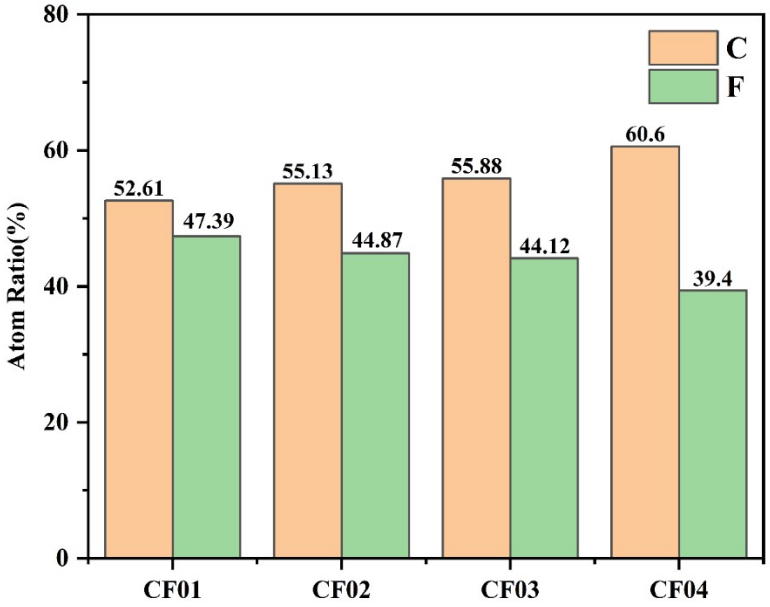

Fig. S3. Atomic ratios of C and F elements in CF01, CF02, CF03, and CF04.

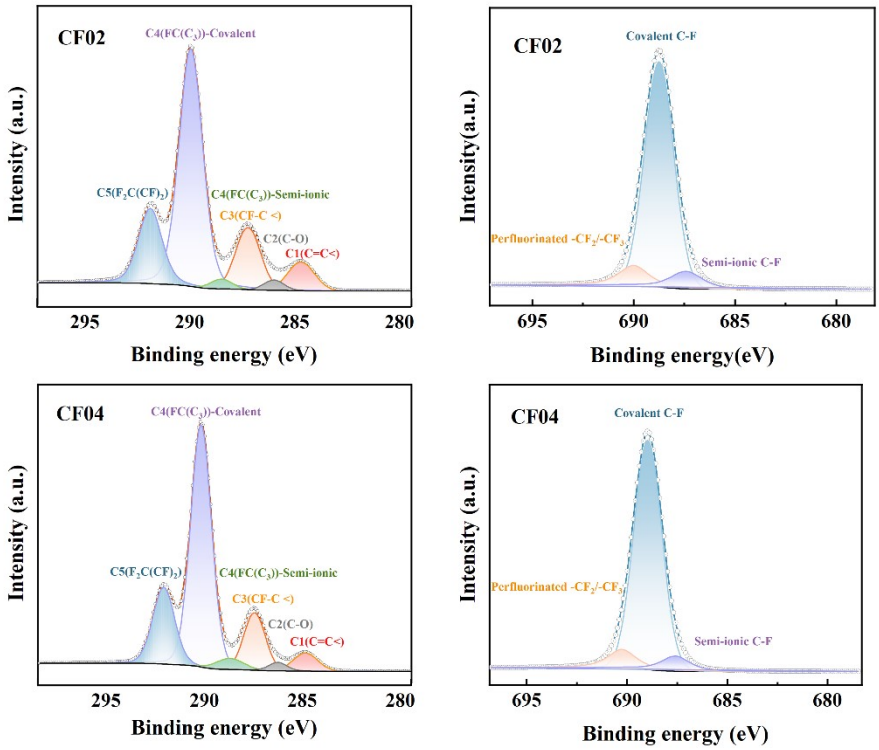

Fig. S4 XPS spectra of C 1s and F 1s for CF02 and CF04

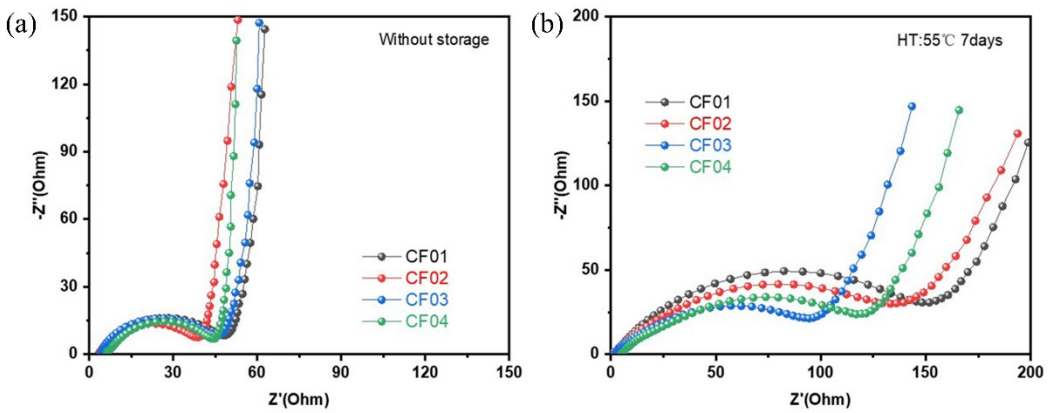

Fig. S5. EIS Nyquist plots of CF01, CF02, CF03, and CF04 coin cells before and after storage.

Mass spectra showing the presence of aldehydes, ketones, and other species in the electrolyte after storage. ^{19}F NMR confirms the presence of HF.

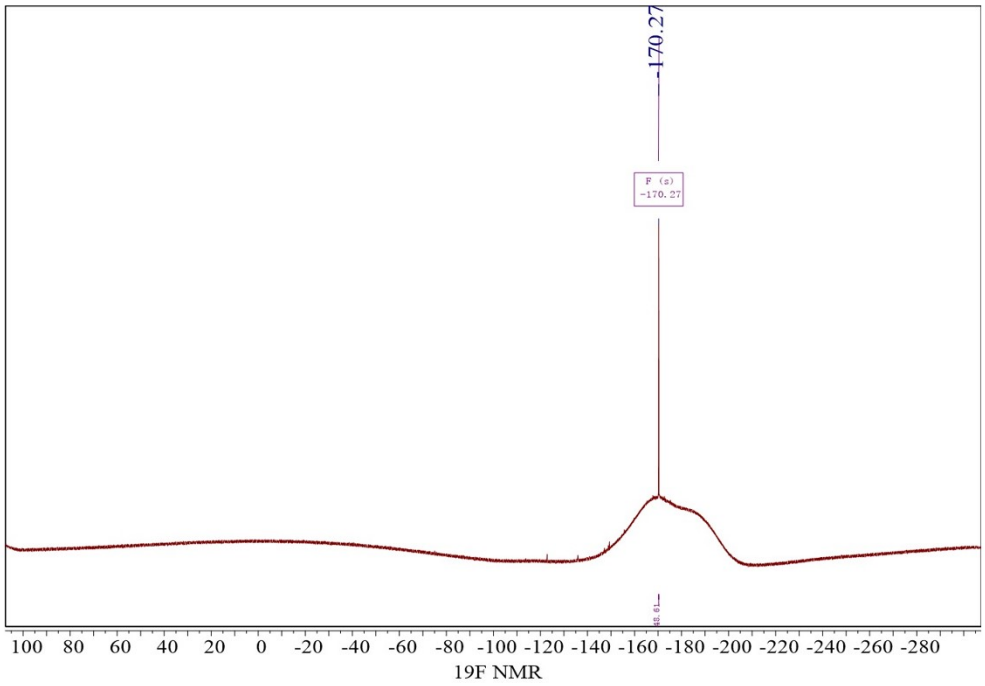

Fig. S6. ^{19}F NMR spectra of the electrolyte after storage at 55°C for 7 days.

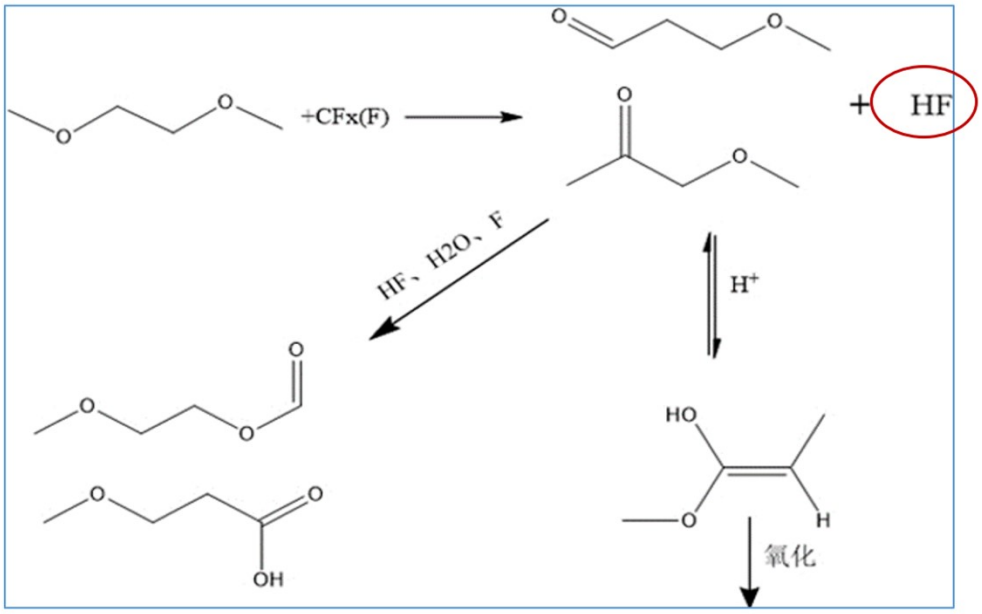

Fig. S7. Schematic diagram illustrating the reaction pathway for HF generation.

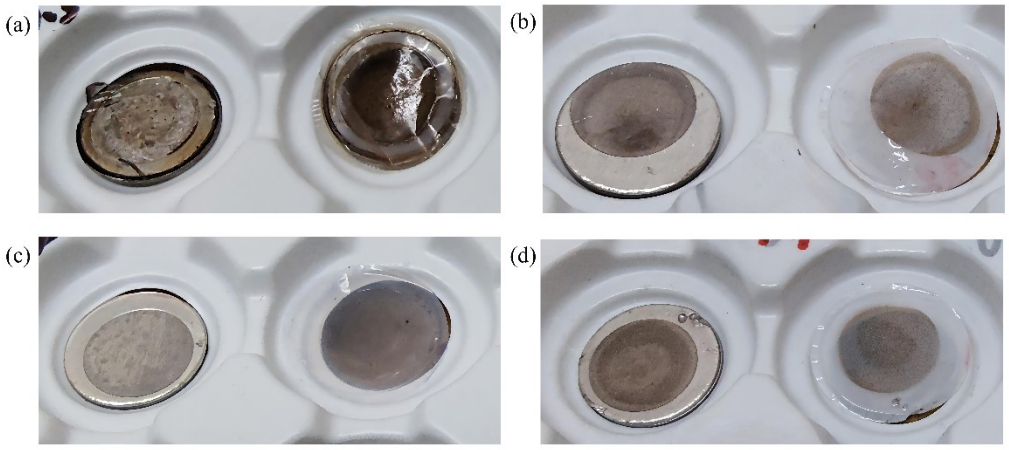

Fig. S8. (a-d) Optical images of the lithium metal anode (left) and separator (right) in the Li/CFx (CF01, CF02, CF03, CF04) battery after storage at 55° C for 7 days.

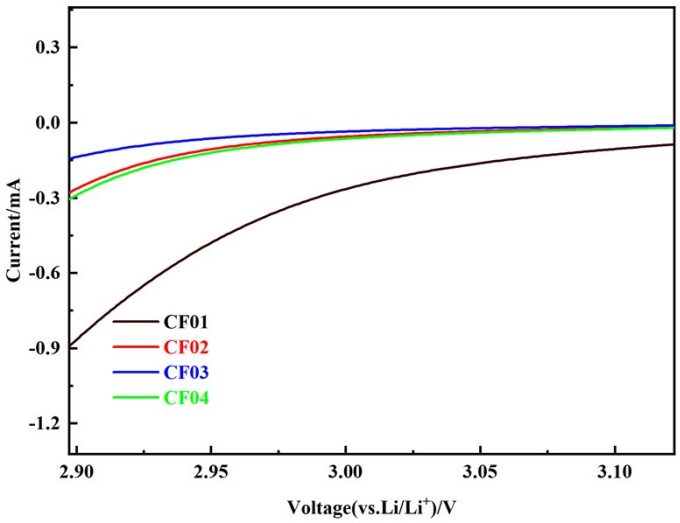

Fig. S9. Enlarged view of the LSV curves for CF01, CF02, CF03, and CF04.

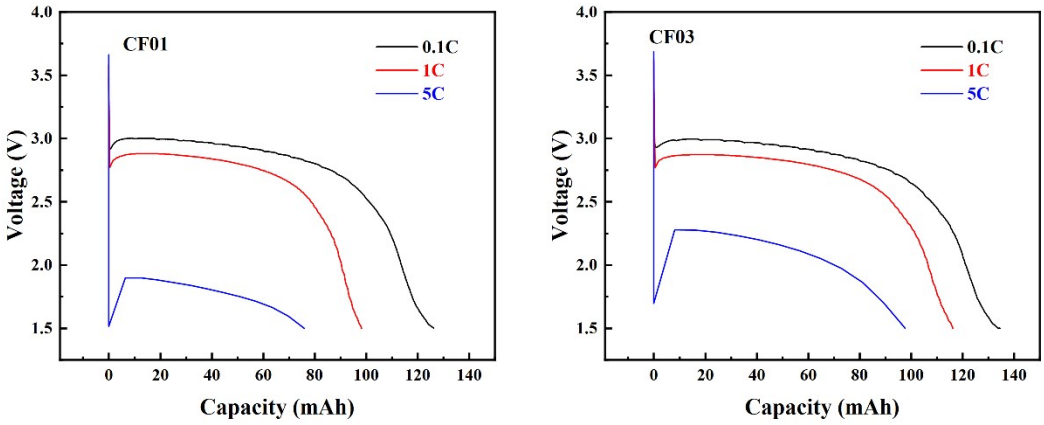

Fig. S10. Discharge curves of the CF01 and CF03 pouch cells at various rates (0.1C, 1C, and 5C) after storage.

Tab. 1. Binding energies and surface elemental compositions of CF01, CF02, CF03, and CF04 obtained from XPS analysis.

		Peak position/eV	CF01	CF02	CF03	CF04
C1s	C=C<	284.76	4.30	3.99	4.69	4.93
	C-O	286.08	1.80	2.00	1.98	1.90
	CF-C <	287.46	15.71	12.90	13.55	13.27
F1s	Covalent C-F	688.97	80.03	82.09	83.45	83.00
	Perfluorinated-CF_2/-CF_3	690.3	10.32	10.10	9.32	9.58
	Semi-ionic C-F	687.64	9.64	7.82	7.23	7.42

Tab. 2. Reduction potentials of CF01, CF02, CF03, and CF04.

	CF01	CF02	CF03	CF04
Reduction potentials(vs.Li/Li^+)/V	3.47	3.43	3.39	3.42

Tab. 3. Other electrochemical performances of CF01 and CF03.

	Gravimetric energy density (Wh kg^{-1})	Gravimetric power density (W/kg)	Average discharge voltage (V)
CF01	475.00	209.93	2.73
CF03	468.84	210.05	2.74